Available online at www.pelagiaresearchlibrary.com

Pelagia Research Library

Advances in Applied Science Research, 2012, 3 (4):2169-2178

ISSN: 0976-8610
CODEN (USA): AASRFC

Hydromagnetic oscillatory flow through a porous medium bounded by two vertical porous plates with heat source and soret effect

K. Chand[1], R. Kumar[2] and S. Sharma[3]

[1]Department of Mathematics and Statistics, H.P.U-Shimla, India
[2]Depatrment of Mathematics, Govt. College for Girls (RKMV) - Shimla, India
[3]Department of Mathematics and Statistics, H.P. U-Shimla, India

---

ABSTRACT

An oscillatory hydromagnetic flow through a porous medium bounded by two vertical parallel porous plates is analyzed. One plate of the channel is kept stationary and the other is moving with uniform velocity. The plates of the channel are subjected to constant injection and suction velocities respectively. By considering the heat source and the Soret effects, closed form solutions of the governing equations are obtained for the velocity, the temperature and the concentration profiles. The effects of the various parameters entering into the problem on the velocity, the temperature, the skin friction and the rate of heat and the mass transfer coefficient are numerically evaluated and discussed with the help of graphs and tables.

Keywords: Hydromagnetic, Oscillatory, Porous medium, Heat source, Soret effect.

Nomenclature

$B_0 =$ Electromagnetic induction

$C_p =$ Specific heat at the constant pressure

$d =$ Distance between the plates

$D_a = \frac{K^* V_0}{\upsilon d} =$ Darcy number

$g =$ Acceleration due to gravity

$G_r = \frac{g\beta\nu(T_w^* - T_0^*)}{UV_0^2} =$ Grashoff number

$G_m = \frac{g\beta_c\nu(C_w^* - C_0^*)}{UV_0^2} =$ Modified Grashoff number

$K =$ Porous medium permeability coefficient

$M = B_0 d\sqrt{\frac{\sigma}{\mu}} =$ Hartmann number

$p =$ Non − dimensional pressure

$R_e = \frac{V_0 d}{\upsilon} =$ Reynolds number

$S = \frac{Q^*\upsilon}{\rho C_p V} =$ Heat source parameter

$S_0 = \frac{D_1(T_w^* - T_0^*)}{\upsilon(C_w^* - C_0^*)} =$ Soret number

$S_c = \frac{\nu}{D} =$ Schmidt number

$t =$ Non − dimensional time coordinate

$u =$ Non − dimensional velocity

$U =$ Uniform velocity of the plate

$V_0 =$ Constant suction/injection

$x =$ Axial space coordinate

$\omega =$ Frequency of oscillations

$\upsilon = \frac{\mu}{\rho} =$ Kinematic viscosity

$\sigma =$ Conductivity of the fluid

$\theta =$ Non − dimensional temperature

INTRODUCTION

The flows through porous media are very much prevalent in nature and therefore, the study of such flows has become of principal interest in many scientific and engineering applications. This type of flows has shown their great importance in petroleum engineering to study the movements of natural gas, oil and water through the oil reservoirs; in chemical engineering for the filtration and water purification processes. Further, to study the underground water resources and seepage of water in river beds one need the knowledge of the fluid flow through porous medium. Therefore, there are number of practical uses of the fluid flow through porous media. The porous medium is in fact a non-homogeneous medium but for the sake of analysis, it may be possible to replace it with a homogeneous fluid which has dynamical properties equal to those of non-homogeneous continuum. Thus one can study the flow of hypothetical fluid under the action of the properly averaged external flow and the complicated problem of the flow through a porous medium reduces to the flow problem of homogeneous fluid with some additional resistance. Ahmadi and Manvi [1] have derived the general equation of motion and applied the results to some basic flow problems. Ram and Mishra [5] applied these equations to study the MHD flow of conducting fluid through porous media. The hydrodynamic channel, which is a classical problem; the exact solution is obtained by Schlichting [11]. A series of investigations have been made by different scholars where the porous medium is either bounded by a channel or by a plane surface [Raptis (9), Raptis and Perdikis (10), Singh *et al* (17)]. The three dimensional Couette flow through porous media has been studied by Singh and Sharma [16]. Ali and Mehmood [2] studied the homotopy analysis of unsteady boundary layer flow adjacent to a permeable stretching surface in a porous medium.

On the other hand, in view of increasing technical applications using magnetohydrodynamics (MHD) effects, it is desirable to extend many of the available hydrodynamic solutions to include the effects of magnetic field for those cases where the viscous fluid is electrically conducting. The various applications of MHD flows in technological fields have been compiled by Moreau [7]. Heat transfer in three dimensional MHD flow past a porous plate subjected to sinusoidal transverse suction velocity has been analyzed by Singh *et al* [14]. Sharma and Sharma [12] have studied the effect of oscillatory suction and heat source on heat and mass transfer in MHD flow along a vertical porous plate bounded by porous medium. Singh and Mathew [15] have studied the injection/ suction effect on an oscillatory hydromagnetic flow in a rotating horizontal porous channel. Gaikwad and Rahuldev [18] studied effects of viscous dissipation of permeable fluid on laminar flow in a channel.

In processes such as drying, evaporation at the surface of water body, energy transfer in a wet cooling tower and the flow in a desert cooler, heat and mass transfer occurs simultaneously. Heat transfer for an electrically conducting fluid flow under the influence of magnetic fields are considered significant due to its applications in many engineering problems such as nuclear reactors and those dealing with liquid metals. Eckert and Drake [4] have pointed out that when a convective flow of the mass is caused by temperature difference one cannot neglect the thermal diffusion effect which is commonly known as Soret effect due to its practical applications in engineering and science. Raju *et al* [8] studied Soret effect due to natural convection between heated inclined plates. Hurle and Jakeman [6] have discussed the effect of a temperature gradient on the diffusion of a binary mixture. Recently Singh and Garg [13] have studied the radiative heat transfer in MHD oscillatory flow through porous medium bounded by two vertical porous plates. The objective of this paper is to analyze the heat source and the Soret effect on an oscillatory hydromagnetic flow of a viscous, incompressible and electrically conducting fluid through saturated porous medium bounded by two parallel porous plates.

MATHEMATICAL ANALYSIS

Consider the flow of an electrically conducting, viscous incompressible fluid through saturated porous medium bounded by two insulated vertical porous plates distance‘d’ apart in the presence of the heat source. A coordinate system is chosen with origin at the stationary plate which is subjected to a constant injection velocity V_0. The other plate moves with uniform velocity U and is subjected to same constant suction velocity V_0. A homogeneous magnetic field of strength B_0 is applied normal to the plane of the plates as shown in the Fig.1.The plates of the channel are assumed infinite in extent hence all the physical properties of the fluid will be function of y^* and t^* except the pressure. Under the usual Boussinesq approximations the flow is governed by the following equations.

$$\frac{\partial v^*}{\partial y^*} = 0, \quad \Rightarrow \; v^* = V_0 \quad , \tag{1}$$
$$\frac{\partial u^*}{\partial t^*} + v^*\frac{\partial u^*}{\partial y^*} = -\frac{1}{\rho}\frac{\partial p^*}{\partial x^*} + \nu\frac{\partial^2 u^*}{\partial y^{*2}} - \frac{\upsilon}{K^*}u^* - \sigma\frac{B_0^2}{\rho}u^* + g\beta(T^* - T_0^*) + g\beta_c(C^* - C_0^*), \tag{2}$$
$$\frac{\partial T^*}{\partial t^*} + v^*\frac{\partial T^*}{\partial y^*} = \frac{k}{\rho C_p}\frac{\partial^2 T^*}{\partial y^{*2}} + \frac{Q^*}{\rho C_p}(T^* - T_0^*), \tag{3}$$
$$\frac{\partial C^*}{\partial t^*} + v^*\frac{\partial C^*}{\partial y^*} = D\frac{\partial^2 C^*}{\partial y^{*2}} + D_1\frac{\partial^2 T^*}{\partial y^{*2}}. \tag{4}$$

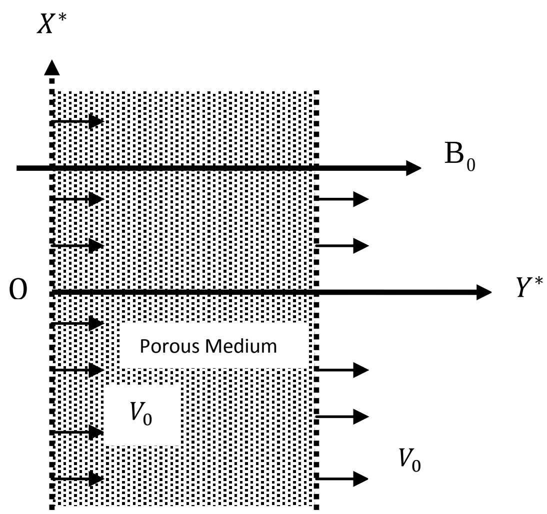

Fig.1: The physical configuration of the problem.

The boundary conditions relevant to the problem are:

$$\left.\begin{aligned} u^* = 0, \quad T^* = T_0{}^*, \; C^* = C_0{}^* \quad &\text{at } y^* = 0 \\ u^* = U, T^* = T_w^*, \; C^* = C_w^* \quad &\text{at } y^* = d. \end{aligned}\right\} \tag{5}$$

On introducing the following Non-dimensional parameters

$$\begin{aligned} &x = \frac{x^*}{d}, \quad y = \frac{y^*}{d}, \quad u = \frac{u^*}{U}, \quad t = t^*\frac{V_0}{d}, \theta = \frac{T^* - T_0^*}{T_w^* - T_0^*}, C = \frac{C^* - C_0^*}{C_w^* - C_0^*}, p = \frac{p^*}{\rho U V_0}, R_e = \frac{V_0 d}{\nu}, \\ &M = B_0 d\sqrt{\frac{\sigma}{\mu}}, P_e = \frac{\rho C_p V_0 d}{k}, \quad D_a = \frac{K^* V_0}{\upsilon d}, G_r = \frac{g\beta\nu(T_w^* - T_0^*)}{U V_0^2}, G_m = \frac{g\beta_c\nu(C_w^* - C_0^*)}{U V_0^2}, \\ &\omega = \frac{\omega^* d}{V_0}, \quad S = \frac{Q^*\nu}{\rho C_p V}, \quad S_0 = \frac{D_1(T_w^* - T_0^*)}{\upsilon(C_w^* - C_0^*)}, \quad S_c = \frac{\nu}{D} \end{aligned} \tag{6}$$

in equations (1) to (4), we get the following non-dimensional governing equations:

$$\frac{\partial u}{\partial t} + \frac{\partial u}{\partial y} = -\frac{\partial p}{\partial x} + \frac{1}{R_e}\frac{\partial^2 u}{\partial y^2} - \frac{1}{D_a}u - \frac{M^2}{R_e}u + G_r R_e\theta + G_m R_e C, \tag{7}$$
$$\frac{\partial \theta}{\partial t} + \frac{\partial \theta}{\partial y} = \frac{1}{P_e}\frac{\partial^2 \theta}{\partial y^2} + S\theta \tag{8}$$
$$\frac{\partial C}{\partial t} + \frac{\partial C}{\partial y} = \frac{1}{S_c R_e}\frac{\partial^2 C}{\partial y^2} + S_0\frac{\partial^2 \theta}{\partial y^2}. \tag{9}$$

The non-dimensional boundary conditions are:

$$\left.\begin{aligned} u = 0, \quad \theta = 0, \quad C = 0 \quad &\text{at} \quad y = 0 \\ u = 1, \quad \theta = 1, \quad C = 1 \quad &\text{at} \quad y = 1. \end{aligned}\right\} \tag{10}$$

METHOD OF SOLUTION

In order to solve equations (7), (8) and (9) for purely oscillatory flow following Chaudhary *et. al* (3), we assume the solution of the form:

$$-\frac{\partial p}{\partial x} = \lambda e^{i\omega t}, \qquad u(y,t) = u_0(y)e^{i\omega t} \quad \text{and} \quad \theta(y,t) = \theta_0(y)e^{i\omega t}. \tag{11}$$

where λ is a constant and ω is the frequency of oscillation. Using equation (11) in equations (7), (8) and (9) and solving, we obtain the following expression for the velocity, the temperature and concentration profiles

$$u(y,t) = \left\{r_{14}e^{A_6 y} + r_{13}e^{A_5 y} - r_7 e^{A_4 y} - r_8 e^{A_3 y} - r_{12}e^{A_2 y} + r_{11}e^{A_1 y} + \frac{\lambda R_e}{m_3^2}\right\} e^{i\omega t} \tag{12}$$

$$\theta(y,t) = \frac{(e^{A_1 y} - e^{A_2 y})}{e^{A_1} - e^{A_2}} e^{i\omega t} \tag{13}$$

$$C(y,t) = \{r_4 e^{A_4 y} + r_3 e^{A_3 y} + r_2 e^{A_2 y} - r_1 e^{A_1 y}\} e^{i\omega t} \tag{14}$$

Skin-friction, Nusselt number and Sherwood number:

The non-dimensional skin friction at the moving plate of the channel is given by

$$\tau = -\mu\left(\frac{\partial u}{\partial y}\right)_{y=1}$$
$$= \{A_6 r_{14} e^{A_6} + A_5 r_{13} e^{A_5} - A_4 r_7 e^{A_4} - A_3 r_8 e^{A_3} - A_2 r_{12} e^{A_2} + A_1 r_{11} e^{A_1}\} e^{i\omega t} \tag{15}$$

The rate of heat transfer at the moving plate of the channel in terms of non-dimensional Nusselt number is given by

$$N_u = -\left(\frac{\partial \theta}{\partial y}\right)_{y=1} = \left\{\frac{A_2 e^{A_2} - A_1 e^{A_1}}{e^{A_1} - e^{A_2}}\right\} e^{i\omega t} \tag{16}$$

The rate of mass transfer coefficient at the moving plate of the channel in terms of non-dimensional Sherwood number is given by

$$S_h = \left(\frac{\partial C}{\partial y}\right)_{y=1} = \{A_4 r_4 e^{A_4} + A_3 r_3 e^{A_3} + A_2 r_2 e^{A_2} - A_1 r_1 e^{A_1}\} e^{i\omega t} \tag{17}$$

Here

$$A_1 = \frac{P_e + \sqrt{{P_e}^2 + 4m_2^2}}{2}, \quad A_2 = \frac{P_e - \sqrt{{P_e}^2 + 4m_2^2}}{2}, \quad A_3 = \frac{S_c + \sqrt{{S_c}^2 + 4m_1^2}}{2}, \quad A_4 = \frac{S_c - \sqrt{{S_c}^2 + 4m_1^2}}{2},$$

$$A_5 = \frac{R_e + \sqrt{{R_e}^2 + 4m_3^2}}{2}, \quad A_6 = \frac{R_e - \sqrt{{R_e}^2 + 4m_3^2}}{2}, \quad m_1 = \sqrt{i\omega ScR}, \quad m_2 = \sqrt{(i\omega - S)P_e}, \quad m_3 = \sqrt{M^2 + \frac{R}{Da} + i\omega R},$$

$$m_4 = (e^{A_6} - e^{A_2}),\ m_5 = (e^{A_6} - e^{A_1}),\ m_6 = (e^{A_6} - e^{A_3}),\ m_7 = (e^{A_6} - e^{A_4}),\ m_8 = (e^{A_5} - e^{A_1}),$$

$$m_9 = (e^{A_5} - e^{A_2}),\ m_{10} = (e^{A_5} - e^{A_3}),\ m_{11} = (e^{A_5} - e^{A_4}),\quad r_1 = \frac{S_o S_c R_e A_1^2}{(e^{A_1} - e^{A_2})(A_1^2 - S_c R A_1 - m_1^2)},$$

$$r_2 = \frac{S_o S_c R_e A_2^2}{(e^{A_1} - e^{A_2})(A_2^2 - S_c R A_2 - m_1^2)},\ r_3 = \frac{r_1(e^{A_4} - e^{A_1}) + r_2(e^{A_2} - e^{A_4}) - 1}{e^{A_4} - e^{A_3}},\quad r_4 = \frac{1 + r_1(e^{A_1} - e^{A_3}) + r_2(e^{A_3} - e^{A_2})}{e^{A_4} - e^{A_3}},$$

$$r_5 = \frac{G_r R_e^2}{(e^{A_1} - e^{A_2})(A_1^2 - R_e A_1 - m_3^2)},\ r_6 = \frac{G_r R_e^2}{(e^{A_1} - e^{A_2})(A_2^2 - RA_2 - m_3^2)},\quad r_7 = \frac{G_m R_e^2 r_4}{A_4^2 - RA_4 - m_3^2},\quad r_8 = \frac{G_m R_e^2 r_3}{A_3^2 - RA_3 - m_3^2},$$

$$r_9 = \frac{G_m R_e^2 r_2}{A_2^2 - RA_1 - m_3^2},\quad r_{10} = \frac{G_m R_e^2 r_1}{A_1^2 - RA_1 - m_3^2},\quad r_{11} = r_{10} - r_5,\quad r_{12} = r_9 - r_6,$$

$$r_{13} = \frac{m_3^2\{r_{12}m_4 - r_{11}m_5 + r_8 m_6 + r_7 m_7 - 1\} + \lambda R(1 - e^{A_6})}{m_3^2(e^{A_6} - e^{A_5})},\quad r_{14} = \frac{1 + \lambda R(e^{A_5} - 1) + m_3^2\{r_{11}m_8 - r_{12}m_9 - r_8 m_{10} - r_7 m_{11} + 1\}}{m_3^2(e^{A_6} - e^{A_5})}.$$

RESULTS AND DISCUSSION

To discuss the physical significance of various parameters involved in the results (12) to (17), the numerical calculations has been carried out and only the real parts of the results obtained have been considered. Our results are found in agreement with the results of Singh and Garg [13] in the absence of heat source and the mass transfer parameters. The effects of the various parameters entering in the governing equations on the velocity, the temperature, the skin friction, the Nusselt number and the Sherwood number are shown through graphs and tables.

The variations in the dimensionless velocity profiles $u(y,t)$ with y for the various parameters involved in the governing equation are graphically illustrated by Fig. 2 and 3. It is observed from Fig.2, that velocity profiles increase with increasing Reynolds number R_e which is in confirmation with the fact that if R_e is large the inertial forces will be predominant and the effect

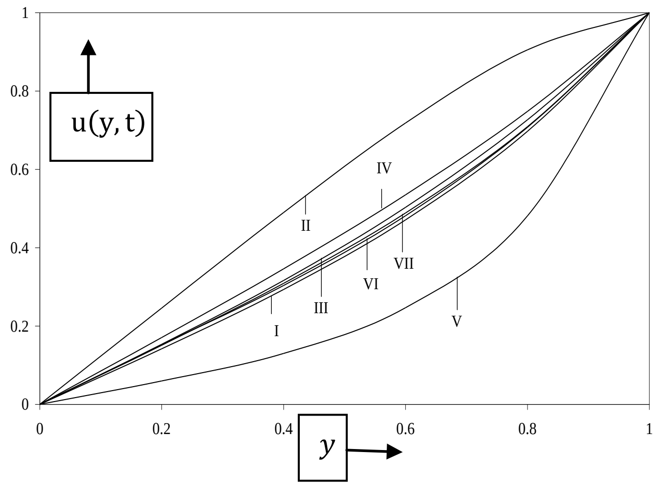

R_e	G_r	G_m	M	S	S_c	Curve
0.5	5	5	2	0.10	0.22	I
1.0	5	5	2	0.10	0.22	II
0.5	10	5	2	0.10	0.22	III
0.5	5	10	2	0.10	0.22	IV
0.5	5	5	4	0.10	0.22	V
0.5	5	5	2	0.80	0.22	VI
0.5	5	5	2	0.10	0.66	VII

Fig. 2: The velocity profiles for $\mathbf{S_0 = 6.89}$ **,** $\mathbf{D_a = 0.5}$, $\mathbf{P_e = 1}$, $\boldsymbol{\omega} \mathbf{= 5}$, $\boldsymbol{\lambda} \mathbf{= 1}$ **and** $\mathbf{t = 0}$

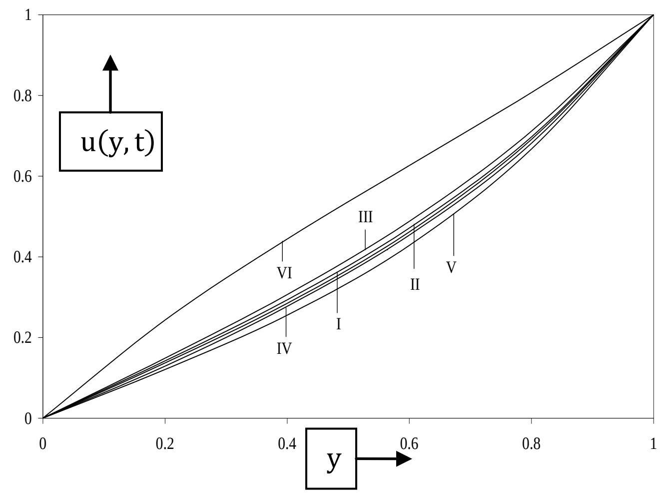

R_e	S_0	D_a	P_e	ω	λ	Curve
0.5	6.89	0.5	1	5	1	I
0.5	2.50	0.5	1	5	1	II
0.5	6.89	1.0	1	5	1	III
0.5	6.89	0.5	5	5	1	IV
0.5	6.89	0.5	1	10	1	V
0.5	6.89	0.5	1	5	5	VI

Fig. 3: The velocity profiles for $\mathbf{G_r = 5}$, $\mathbf{G_m = 5}$, $\mathbf{M = 2}$, $\mathbf{S = 0.10}$, $\mathbf{S_c = 0.22}$ **and** $\mathbf{t = 0}$.

of viscosity will confined only to the thin region adjacent to the solid surface. It is also clear from this Fig. that for heavier species i.e increasing Schmidt number $(S_c = 0.66 - \text{Oxygen and } S_c = 0.22 - \text{Hydrogen})$, the velocity decrease. It is again in agreement, with property of the Schmidt number, which represent the ratio of kinematic viscosity and diffusivity of the diffusing species. Further with the increasing Lorentz force parameter i.e. the Hartmann number M and the heat source parameter S the velocity decrease.

From Fig.3, it is evident that the velocity profiles increase with increasing porous medium permeability D_a and the amplitude of the pressure gradient λ along the channel. Increasing Peclet

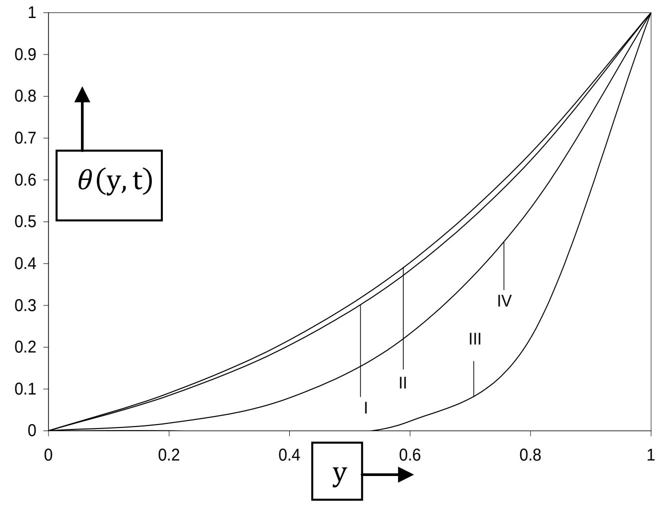

S	P_e	ω	Curve
0.10	1	5	I
0.80	1	5	II
0.10	5	5	III
0.10	1	1	IV

Fig. 4: The temperature profiles.

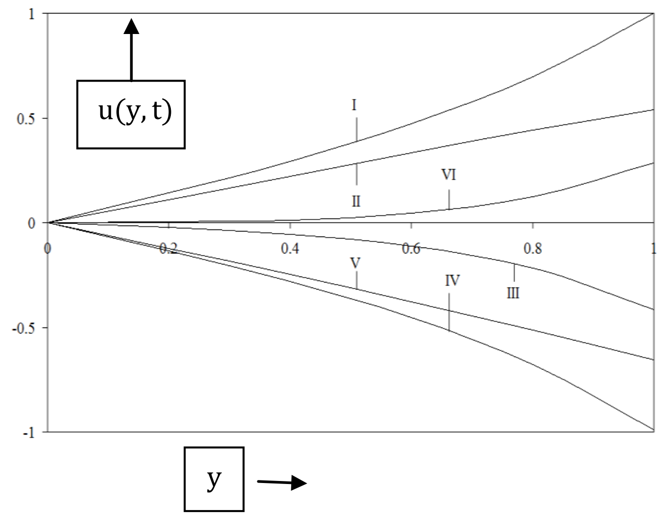

Curve	I	II	III	IV	V	VI
Time(t)	0	0.2	0.4	0.6	0.8	1

Fig.5: The velocity profiles for $G_r = 5$, $G_m = 5$, $M = 2$, $S = 0.10$, $S_c = 0.22$, $S_0 = 6.89$, $D_a = 0.5$, $P_e = 1$, $\omega = 5$ and $\lambda = 1$ with time.

number P_e and frequency of oscillation ω adversely affect the velocity profiles. Moreover it is observed that velocity profiles are more for the thermal diffusion ratio of $(H_2 - CO_2)$, $S_0 = 6.89$ as compared to the thermal diffusion ratio of $(He - Ar)$, $S_0 = 2.50$.

The variation in temperature profile $\theta(y, t)$ with y for the various parameters involved is illustrated by Fig. 4. It is clear from this Fig. that temperature profile increase with increasing heat source parameter S and the frequency of oscillation ω and it decrease with the increasing P_e .

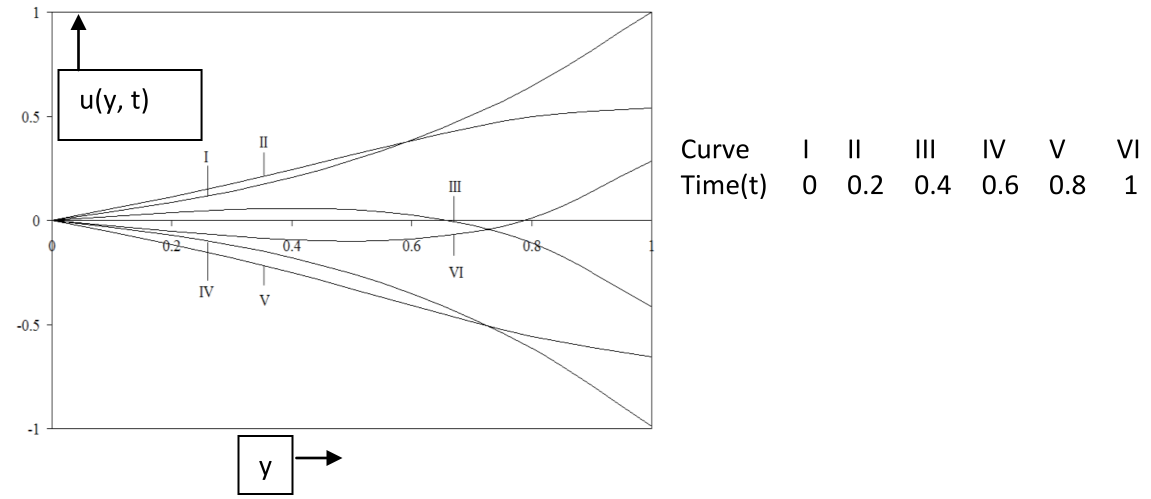

Fig. 6: The temperature profiles for $P_e = 1, S = 0.10, \omega = 5$ with time.

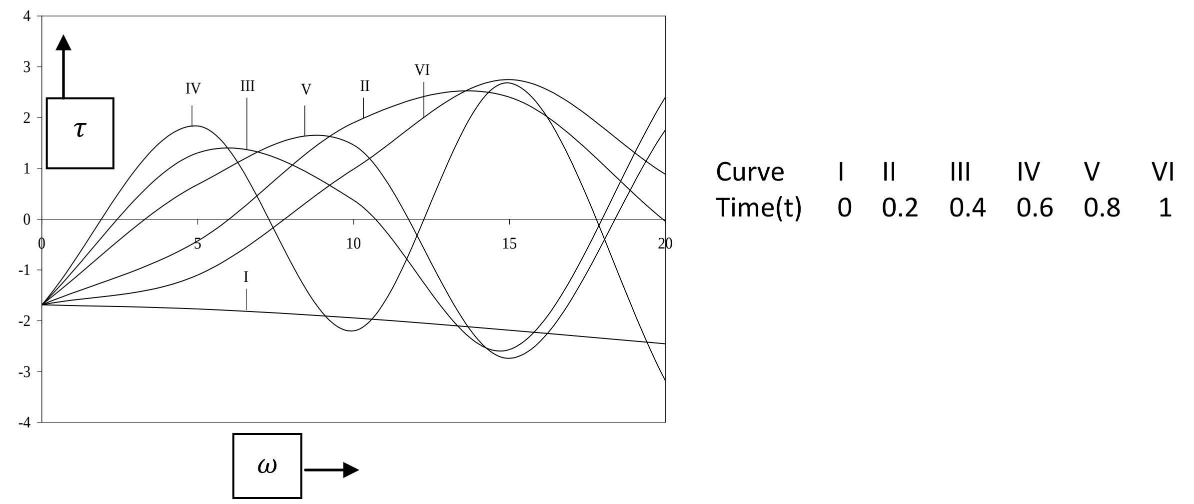

Fig.7: Variation of the skin friction $R_e = 0.5$, $G_r = 5, G_m, = 5, M =, 2\ S_0 = 6.89,$ $S_c = 0.22$, $D_a = 0.5, P_e = 1$, $\lambda = 1$ and $y = 1$ with time.

The variations in the skin friction profiles τ with the frequency of oscillation ω are given in the Tables 1 and 2. It is observed from the Table 1, that the skin friction profile is enhanced with the increasing Reynolds number R_e, the Grashoff number G_r, the modified Grashoff number G_m, and Soret number S_0 and velocity reduces with the Hartmann number M.

It is observed from Table 2, that the skin friction is enhanced with Schmidt number S_c, Darcy number D_a and the amplitude of the pressure gradient. The increase in the frequency of oscillation ω and the Peclet number P_e leads to reduce the skin friction.

The tabular illustration of the variations in the dimensionless rate of heat transfer i.e the Nusselt number N_u is depicted in Table 3. It can be interpreted from this Table that the rate of heat

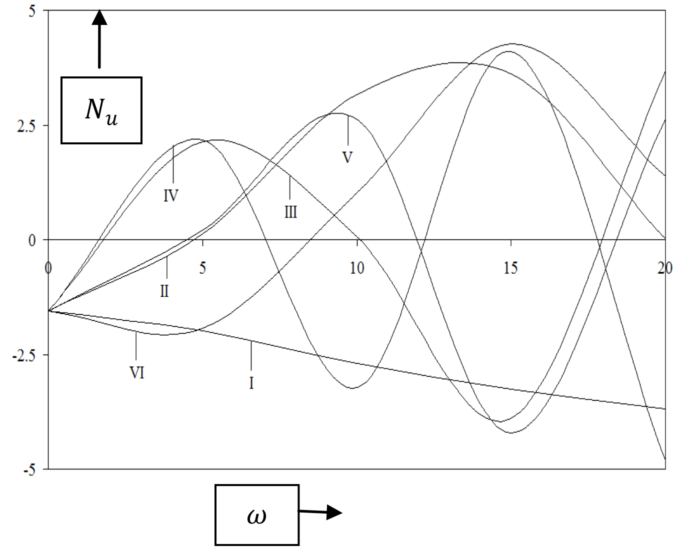

Fig.8: Variation of the Nusselt number for $P_e = 1$, $S = 0.10$ with time.

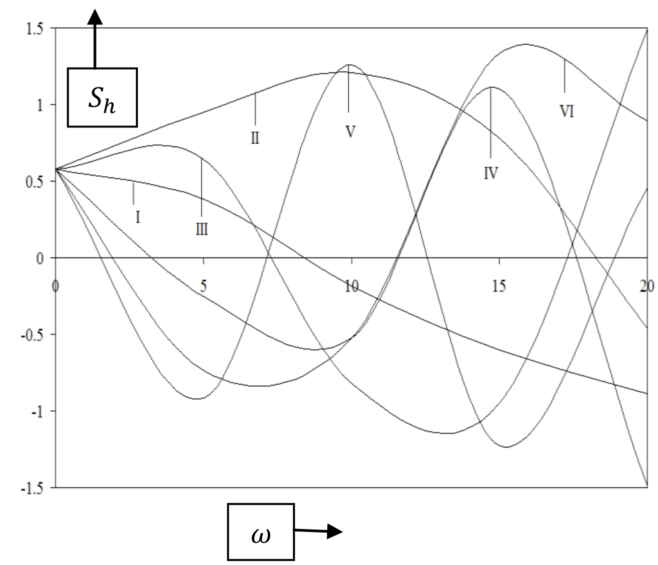

Fig.9: Variation of the Sherwood number for R_e =0.5, $S_0 = 6.89$, $S_c =.22$ at $y = 1$ with time.

transfer is slightly increased for the large value of Peclet number P_e whereas the increase in the heat source parameter S leads to reduction in the heat transfer.

The Table 4, represent the variation in the dimensionless rate of mass transfer coefficient i.e the Sherwood number S_h . It is evident from this Table that the rate of mass transfer coefficient is reduced with the Reynolds number R_e, the Schmidt number S_c and the Soret number S_0.

Figs. 5 to 9 show the variations in the velocity profiles, the temperature profiles, the skin friction, the Nusselt number and the Sherwood number respectively with time. As expected there is periodic variation in these profiles with time and the amplitude of these variations increases with increasing frequency of oscillation. The pattern of these variations is repeated for higher value of time.

CONCLUSION

The conclusions of the study are:

- The Lorentz force parameter i.e. the Hartmann number contributes to reduce the velocity and the skin friction profiles.
- The effect of the permeability parameter i.e. Darcy number is just opposite to that of Lorentz force parameter.
- For the species with large diffusion ratio the velocity is enhanced and skin friction is reduced.
- The heat transfer is reduced with heat generation parameter.
- The rate of mass transfer is less for the fluid with large viscosity.

Table- 1: Skin friction at S_0=6.89, S_c=0.22, D_a=0.5, P_e=1.0, λ=5.0, $t = 0$.

R	G_r	G_m	M	S	$\omega = 0$	$\omega = 10$	$\omega = 20$
0.5	5	5	2	0.10	-1.4341	-1.2273	-0.84954
1.0	5	5	2	0.10	-2.5146	-1.8353	-0.86128
0.5	10	5	2	0.10	-1.5201	-1.2387	-0.82944
0.5	5	10	2	0.10	-1.5701	-1.3813	-0.95776
0.5	5	5	4	0.10	-0.7706	-0.7274	-0.64106
0.5	5	5	2	0.80	-1.4267	-1.2272	-0.84921

Table-2: Skin-friction at R=0.5, G_r=5, G_m=5, M=2, S=0.10, $t = 0$.

S_0	S_c	D_a	P_e	λ	$\omega = 0$	$\omega = 10$	$\omega = 20$
6.89	0.22	0.5	1.0	5.0	-1.4341	-1.2273	-0.84954
2.50	0.22	0.5	1.0	5.0	-1.4161	-1.1855	-0.81194
6.89	0.66	0.5	1.0	5.0	-1.4165	-1.3055	-0.84493
6.89	0.22	1.0	1.0	5.0	-1.4895	-1.2628	-0.85594
6.89	0.22	0.5	5	5.0	-1.4082	-1.2185	-0.84825
6.89	0.22	0.5	1.0	1.0	-0.7633	-0.6047	-0.32722

Table-3: For Nusselt number at $t = 0$.

P_e	S	$\omega = 0$	$\omega = 10$	$\omega = 20$
1.0	0.10	-1.5495	-2.6921	-3.6855
5.0	0.10	-4.9379	-7.7950	-9.7772
1.0	0.80	-1.3096	-2.6096	-3.6328

Table-4: For Sherwood number at $t = 0$.

R_e	S_0	S_c	$\omega = 0$	$\omega = 10$	$\omega = 20$
0.5	6.89	0.22	0.92053	-0.12536	-0.85107
1.0	6.89	0.22	0.62658	-1.5550	-2.7524
0.5	2.50	0.22	1.0438	0.6812	0.46631
0.5	6.89	0.66	1.0643	-2.0732	-3.4587

REFERENCES

[1] Ahmadi G, Manvi R, *Indian Journal of Technology*, **1971**, 9, 441-444.
[2] Ali A, Mehmood A, *Communications, in Nonlinear Science and Numerical Simulation*, **2008**, 13, 340-349.
[3] Chaudhary R C, Jha A K, Dhayal S S, *J. Rajasthan Acad. Phy. Sci*., **2006**, 5(2), 233-238.
[4] Eckert E R G, Drake R M, Analysis of heat and mass transfer, New York, Mc Graw Hill, **1972**.
[5] Ram G, Mishra R S, *Indian J. Pure Appl. Math*., **1977**, 8, 637-647.
[6] Hurle D T J, Jakeman E, *J. Fluid Mech*., **1971**, 47(4), 667-687.
[7] Moreau R, Magnetohydrodynamics, Kluwer, Academic Publisher, Dordrecht, **1990**.
[8] Raju M C, Varma S V K, Reddy P V, Saha S, *Journal of Mechanical Engineering*, **2008**, 39, 65-70.
[9] Raptis A, *Int. J. Engng. Sci*., **1983**, 21(4), 345-348.
[10] Raptis A, Perdikis C P, *Int. J. Engng. Sci*., **1985**, 23(1), 51-55.
[11] Schlichting H, Boundary Layer Theory, McGraw-Hill, New York, **1979**.
[12] Sharma P R, Sharma K, *Mod. Meas. & Control 'B', ASME J. France*, **2007**, 76(5), 34-60.

[13] Singh K D Garg B P, *Bull. Cal. Math. Soc*. **2010**, 102(2), 129-138.
[14] Singh K D, Chand K, Rana S K, *Indian J. Pure Appl. Math*., **1993**, 24(5), 327-335.
[15] Singh K D, Mathew A, *Indian Journal of Physics*, **2008**, 82, 435-445.
[16] Singh K D, Sharma R, *Indian J. Pure Appl. Math*, **2001**, 32(12), 1819-1829.
[17] Singh P, Sharma V P, Misra U N, *Int. J. Heat Mass Transfer*, **1978**, 21(8), 1117-1123.
[18] Gaikwad S N, Rahuldev B M, *Advances in appl. Sci. Res*., **2012**, 3(2), 720-734.